energies

MDPI

Article

Projected Changes in Solar PV and Wind Energy Potential over West Africa: An Analysis of CORDEX-CORE Simulations

Aissatou Ndiaye [1,*], Mounkaila Saley Moussa [1,2], Cheikh Dione [3], Windmanagda Sawadogo [4], Jan Bliefernicht [4], Laouali Dungall [2] and Harald Kunstmann [4,5]

1 West African Science Service Center on Climate Change and Adapted Land Uses (WASCAL) Doctoral Research Program in Climate Change and Energy (DRP-CCE), Abdou Moumouni University, Niamey BP 10662, Niger
2 Department of Physics, Faculty of Sciences and Techniques, Abdou Moumouni University, Niamey BP 10662, Niger
3 Institut Pierre Simon Laplace, CNRS, Ecole Polytechnique de Paris, Institut Polytechnique de Paris, CEDEX, 91128 Palaiseau, France
4 Regional Climate and Hydrology, Institute of Geography, University of Augsburg, 86135 Augsburg, Germany
5 Institute of Meteorology and Climate Research, Karlsruhe Institute of Technology, Campus Alpin, 82467 Garmisch-Partenkirchen, Germany
* Correspondence: ndiaye.a@edu.wascal.org

Abstract: Renewable energy development is growing fast and is expected to expand in the next decades in West Africa as a contribution to addressing the power demand and climate change mitigation. However, the future impacts of climate change on solar PV and the wind energy potential in the region are still unclear. This study investigates the expected future impacts of climate change on solar PV and wind energy potential over West Africa using an ensemble of three regional climate models (RCMs). Each RCM is driven by three global climate models (GCMs) from the new coordinated high-resolution output for regional evaluations (CORDEX-CORE) under the RCP8.5 scenario. Two projection periods were used: the near future (2021–2050) and the far future (2071–2100). For the model evaluation, reanalysis data from ERA5 and satellite-based climate data (SARAH-2) were used. The models and their ensemble mean (hereafter Mean) show acceptable performance for the simulations of the solar PV potential, the wind power density, and related variables with some biases. The Mean predicts a general decrease in the solar PV potential over the region of about −2% in the near future and −4% in the far future. The wind power density (WPD) is expected to increase by about 20% in the near future and 40% in the far future. The changes for solar PV potential seem to be consistent, although the intensity differs according to the RCM used. For the WPD, there are some discrepancies among the RCMs in terms of intensity and direction. This study can guide governments and policymakers in decision making for future solar and wind energy projects in the region.

Keywords: CORDEX-CORE; regional climate modelling; climate change; renewable energy; West Africa

Citation: Ndiaye, A.; Moussa, M.S.; Dione, C.; Sawadogo, W.; Bliefernicht, J.; Dungall, L.; Kunstmann, H. Projected Changes in Solar PV and Wind Energy Potential over West Africa: An Analysis of CORDEX-CORE Simulations. *Energies* **2022**, *15*, 9602. https://doi.org/10.3390/en15249602

Academic Editor: Muhammad Asif

Received: 20 October 2022
Accepted: 10 December 2022
Published: 17 December 2022

Publisher's Note: MDPI stays neutral with regard to jurisdictional claims in published maps and institutional affiliations.

1. Introduction

Global energy demand is increasing driven by income and population growth. The US Energy Information Administration expects a 47% increase by 2050 [1]. Currently, fossil fuels remain the dominant source, 80% of energy demand is met by fossil fuels, and the energy system is the source of approximately two-thirds of the world's CO_2 emissions [2]. These fuels are associated with the degradation of the environment by releasing greenhouse gases (GHG) into the atmosphere through their combustion. The increase in the concentration of GHG changes the atmosphere's radiative equilibrium and is considered to be the principal driver of the observed changes in hot and cold extremes on the global scale and most continents [3].

Many African countries are promoting renewable energy in the framework of climate change mitigation. Renewable energy sources (RES) play a role in providing energy services

in a sustainable manner [4]. RES derive their energy directly from the Sun or the heat in the Earth's interior and are thus constantly being renewed. Among the RESs currently used in power generation, solar and wind are the most promising and used [5].

Global renewable energy capacity is expected to expand by 50% between 2019 and 2024, led by solar photovoltaic (PV) [5]. Based on this projection, solar PV represents nearly 60% and onshore wind 25%. The sub-Saharan Africa region is forecasted to add 22 GW of renewable energy capacity during the period 2019–2024 [5]. For example, Senegal implemented more than eight solar plants since 2016 and has the largest wind farm in West Africa, with a capacity of 158.7 MW. Nevertheless, the energy sector, especially renewable, is highly dependent on weather and climate conditions, which affect energy supply and use, energy demand, transport, distribution, and markets. Some of the key environmental effects of climate change are an increase in global surface temperature, changes in hydrological cycles, a rise in mean sea level and a higher incidence of extreme weather events. The disruption to electricity production and supply is expected to be significant as a result of these environmental changes [6]. For this reason, it is important to assess and quantify the magnitude of changes in climate variables that will affect future energy systems, both from a climate and energy perspective, especially in the renewable energy sector [7].

To date, there are several studies on the potential impacts of climate change on solar and wind energy resources and the results depend on the region. Two approaches are widely used to verify or project these changes: using long-term historical data (reanalysis, satellite, climate models or ground data) or using climate models for future changes. A review of potential mechanisms by which global climate variability and change may affect wind resources and operating conditions revealed changes in wind shear, intensity, and duration [8]. Studies for Europe using an ensemble of regional climate models Tobin et al. [9], showed that changes in wind power potential will remain within $\pm$15 and $\pm$20% over most European countries by the mid and late centuries, respectively. Using the Coupled Model Intercomparison Project Phase 5 (CMIP5) projections for solar PV, Müller et al. [10] observed positive impacts for most European countries with only minor adverse impacts in the Nordic countries. In the United States, Breslow and Sailor [11] and Crook et al. [12] projected a reduction in wind speed of up to 5% by 2050 and 2100, and a decrease in the PV output over the Western USA (~3%) by 2100, respectively. In contrast in Brazil, solar resources are expected to increase by 3.6% and wind potential by 40% by the end of the century, especially in the Northeast [13]. In the last few years, studies over Africa on the same topic are becoming more numerous. Sawadogo et al. [14] and Soares et al. [15] projected, respectively, an increase in wind power density in the near and mid-century under RCP2.5 and RCP8.5 over Africa and an increase in wind energy density in the northern regions (<+10%) and a decrease (>−10%) in the southern region of Africa. Studies over West Africa found an increase in wind speed and wind power density Sawadogo et al. [16], while Ogunjobi et al. [17] found a possible decrease in energy produced that can reach 12% in the period 2021–2050 and an increase (~24–30%) in energy production in 2071–2100. On the other hand, using different climate models to assess future solar resources, a general decrease with different magnitudes of PV potential was found over West Africa [18–21].

In the mid-2010s, the CORDEX-CORE initiative was launched by Gutowski et al. [22] to better address the problem of dissimilarity in the size and simulation setup of the projections in different CORDEX domains. The CORDEX-CORE simulations furnish a homogeneous set of projections for all CORDEX domains using a core set of RCMs driven by a common set of GCMs. The model horizontal grid spacing is 25 km $\times$ 25 km, i.e., a resolution four folded compared to the previous CORDEX simulations [23]. Studies on the subject of this investigation over West Africa using an ensemble of RCMs from CORDEX-CORE are very few, if not non-existent, to our knowledge. The existing CORDEX-CORE studies for the African region mainly deal with other variables and processes such as precipitation, dry and wet spell, low-level jets, etc. [24–27].

The objective of this study is therefore to investigate the projected future impacts of climate change on solar and wind energy potential over West Africa using the high-resolution RCM simulations from CORDEX-CORE under the RCP8.5 scenario. As stated above, the projected changes in wind power potential over West Africa are still uncertain, with widely diverging results. We use an ensemble of GCM-RCM combinations to better explore the inherent uncertainties of climate projections for the target variables of this study. As stated by Tebaldi and Knutti [28], the ensemble mean of a multi-model approach in climate modelling often presents fewer biases compared to the individual models, especially for first-order statistics. Moreover, the new high-resolution (25 km) CORDEX-CORE climate models could provide significant added value in terms of spatial resolution as compared to the standard simulations of the CORDEX initiative, which were conducted in 50 km resolution. The study is complemented by a detailed model evaluation of the RCMs for the target variables using state-of-the-art reanalysis and satellite global datasets as reference products.

The following section provides a description of the CORDEX-CORE simulations and the methodology used. The model evaluation results and the projected changes are discussed in Section 3. Section 4 presents the conclusion of the study.

2. Materials and Methods

2.1. Study Area

The study region ranges from 0° N to 25° N and −20° W to 20° E, and includes all West African countries (Figure 1). The region is endowed with renewable energy potential with a high solar energy resources availability [29]. The climate of West Africa is strongly determined by the different atmospheric processes of the West African monsoon system [30]. Continental dry air masses from the high-pressure system above the Sahara Desert cause dusty Harmattan winds over most of West Africa from November to February. In the main monsoon period (June to August), humid air masses originating from the Atlantic Ocean bring monsoon rains over most parts of the study region [30]. Both temperature and rainfall and their annual cycle depend on the way in which dry and moist air masses interact over the year [31]. In this study, we consider three different climatic zones of the region, namely the Guinea zone (18° W to 18° E, 4° N to 8° N), the Savannah zone (18° W to 18° E, 8° N to 12° N), and the Sahel zone (18° W to 18° E, 12° N to 16° N) adopted from Abiodun et al. [32]. Similar domains were used by many other RCM studies for this region (e.g., [16,33,34]). The Guinea zone is characterized by a sub-humid climate with average annual rainfall usually between 1250 mm and 3000 mm, and the Savannah is a semiarid zone with average annual rainfall between 750 mm and 1250 mm [35]. Most of the rainfall in the Sahel zone falls in the boreal summer months (June to September) with an annual mean rainfall amount from roughly 750 mm in the south to less than 200 mm in the north [36].

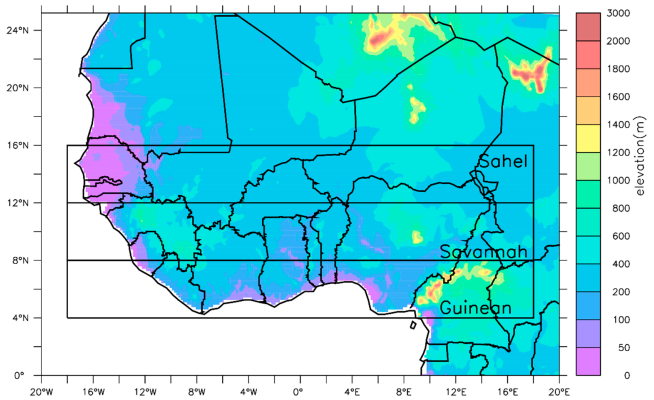

Figure 1. Study area with the three climatic zones (Guinea, Savannah, and Sahel) and the topography in meters (m) in West Africa.

2.2. Data

The data used in this study are the current CORDEX-CORE simulations from the Word Climate Research Program (WCRP), the atmospheric reanalysis dataset (ERA5, [37]), developed by the European Centre for Medium-Range Weather Forecasts (ECMWF), as well as a satellite-based climate dataset (SARAH-2, [38]).

The CORDEX-CORE simulation data used in this study are based on three RCMs namely: RegCM4, REMO, and CCLM, each driven by three GCMs (NorESM1-M, MPI-ESM-MR, and HadGEM2-ES) from the Coupled Model Intercomparison Project 5 (CMIP5, [39,40]). According to Giorgi et al. [41], these GCMs are among the best performing models in the CORDEX domains within the CMIP5 ensemble (e.g., [42,43]). They roughly span the range of global climate sensitivity of the CMIP5 ensemble, with HadGEM2-ES having high sensitivity, and MPI-ESM-MR and NorESM1-M having medium and low sensitivity, respectively, in terms of increase in global mean temperature compared to the pre-industrial level. RegCM4 is the fourth generation version of the RegCM regional modelling system Giorgi et al. [41] developed at the Abdus Salam International Centre for Theoretical Physics (ICTP). REMO is a hydrostatic atmospheric model using hybrid vertical coordinates developed at the Climate Service Center Germany (GERICS) [44,45]. CCLM is a non-hydrostatic model developed by the Consortium for Small-scale Modelling (COSMO) community. In addition, RCMs participating in CORDEX-CORE offer only two RCPs: RCP2.6 and RCP8.5 scenarios [40]. All three RCMs were frequently used for climate simulations in West Africa. Examples are shown by Sawadogo et al. [20] and Kouassi et al. [46] for RegCM, Paeth et al. [47] and Paxian et al. [48] for REMO, and Dosio and Panitz [49] and Dieng et al. [50] for CCLM. To study the future solar PV and wind energy potential, the climate variables taken from the CORDEX-CORE simulations via the ESGF nodes (https://esgf-data.dkrz.de/search/cordex-dkrz/ Accessed on 6 December 2021) are monthly surface downwelling shortwave radiation (RSDS), near-surface air temperature (Tas), and near-surface wind speed at ten meters above ground level (WSPD).

To validate the RCM simulations, monthly surface wind speed (10 m above the ground level) and the ambient air temperature were taken from the ERA5 dataset, which is the fifth generation ECMWF reanalysis for the global climate and weather produced by the Copernicus Climate Change Service at ECMWF. The ERA5 dataset provides estimates of atmospheric variables at a resolution of approximately 31 km worldwide. The monthly shortwave solar radiation was received from the second version of the Surface Solar Radiation Dataset-Heliosat (SARAH-2). SARAH-2 is a satellite-based climate data record of the solar irradiance, the direct irradiance, the sunshine duration, spectral information, and the effective cloud albedo derived from satellite observations of the visible channels of the MVIRI and the SEVIRI instruments onboard the geostationary Meteosat satellites [38]. Details about the quality of this dataset were demonstrated in many studies, including Mueller et al. [51] and Pfeifroth et al. [52]. The SARAH and the ERA5 data cover the period from 1985 to 2014. More details about the model configurations and the data used in this study are given in Table 1.

Table 1. Configuration of the RCMs used in this study in the CORDEX-CORE simulation [53–70].

	RegCM	**REMO**	**CCLM**
Institution	Abdus Salam International Center for Theoretical Physics (ITCP)	Climate Service Centre Germany (GERICS)	Consortium for Small-Scale Modelling (COSMO) community, the German Weather Service (DWD)
Microphysics	SUBEX Pal et al. [53]	Lohmann and Roeckner [61]	Doms et al. [68]
Cumulus convection	Tiedtke and Kain-Fritsch Tiedtke [54] Kain and Fritsch [55]	Tiedtke [54] Nordeng [62] Pfeifer [63]	Tiedtke [54] being modified by D. Mironow (DWD)

Table 1. *Cont.*

	RegCM	REMO	CCLM
Planetary boundary layer	Holtslag Holtslag et al. [56]	Monin-Obukhov similarity theory Louis [64]	Herzog et al. [69]
Radiation scheme	Kiehl et al. [57]	Morcrette et al. [65] Giorgetta and Wild [66]	Ritter and Geleyn [70]
Interactive aerosols	Organic and black carbon, SO4 (Solmon et al. [58]) Dust (Zakey et al. [59]) Sea salt (Zakey et al. [60])	No aerosol module is included. The information about aerosols, for example in the radiation scheme is based on the climatology from Tanre et al. [67].	No aerosol module is included.

SUBEX = Subgrid explicit moisture scheme.

2.3. Methods

Figure 2 indicates the conceptual framework of the study with the two state-of-the global datasets used for RCM evaluation (left side) and the different RCM/GCM combinations of the CORDEX-CORE ensemble (right side). To estimate the solar PV and wind energy potential, the PV potential (PVP) and the wind power density (WPD) are calculated from the respective RCMs and reference datasets. In addition, further variables such as wind speed at 100 m and cell temperature (Tcell) are calculated from the datasets, which are needed for the estimation of the main target variables. Afterwards, a model evaluation of the RCMs of CORDEX-CORE is performed for a 30-year period based on the Mean using the reference datasets. In addition, the projected changes of PVP and WPD are calculated from the CORDEX-CORE ensemble for future periods.

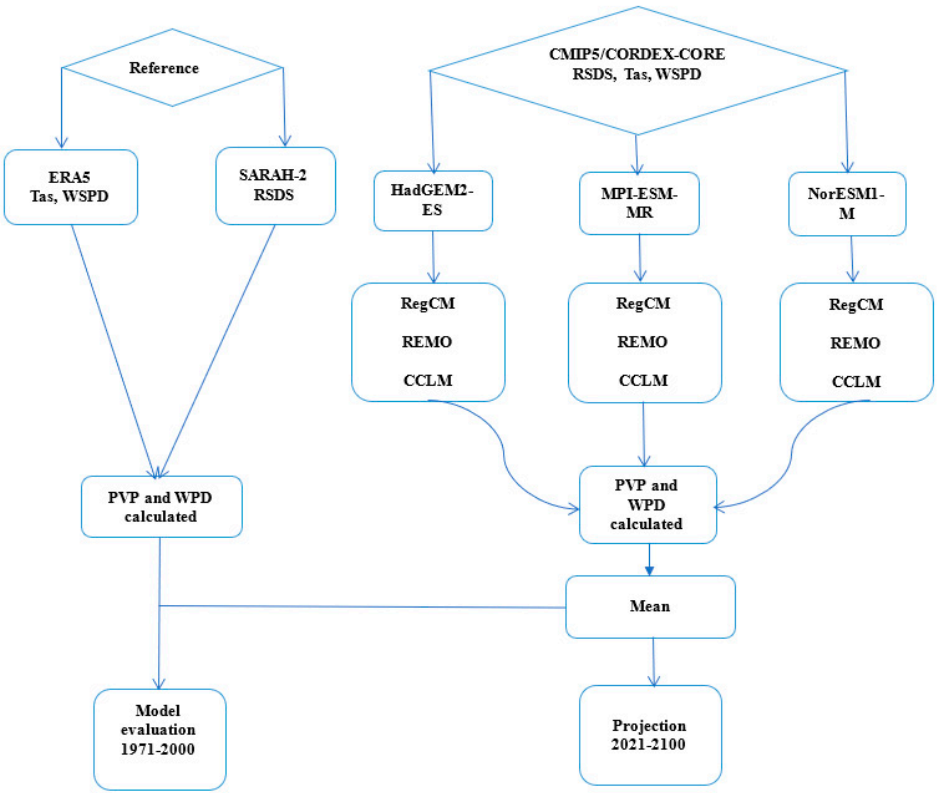

Figure 2. Conceptual framework of the research methodology including the main target variables (e.g., PVP and WPD), the chosen RCMs/GCM combinations of CORDEX-CORE for providing climate projections and the reference datasets used for model evaluation.

2.3.1. Solar PV Potential (PVP)

Photovoltaic potential (PVP) is a value for the expected average electricity production (in kilowatt-hours per kWh) of grid-connected photovoltaic systems without batteries under standard test conditions. The PVP is a function of the performance ratio (Pr) and the RSDS. Pr measures the performance of a PV system and considers environmental factors such as temperature, irradiance, humidity, wind speed, and other meteorological variables. In this study, the PVP is computed following the formula of Mavromatakis et al. [71]. It accounts for the performance of the PV cells in relation to their nominal power according to the actual environmental conditions. This formula was adopted by many studies [16,72–75]. It can be expressed by the Equation (1):

$$PVP = Pr * RSDS \quad (1)$$

where RSDS is the shortwave solar radiation at the location (W m^{-2}) and Pr is the performance ratio, which refers to the changes in PV cell efficiency due to the effect of the cell temperature (T_{Cell}). According to Jerez et al. [72], it can be estimated by using the Equation (2):

$$Pr = 1 + \gamma\,(T_{cell} - T_{STC}) \quad (2)$$

where T_{cell} is the PV cell temperature and T_{STC} is the temperature of the cell under standard test conditions (25 °C). γ is the power thermal coefficient and is equal to 0.005 $°C^{-1}$ for mono-crystalline silicon cells [76]. According to Chenni et al. [77], T_{cell} is usually calculated based on multiple linear regression, considering the effects of the temperature, solar radiation, and wind speed as follows:

$$T_{cell} = C_1 + C_2 * Tas + C_3 * RSDS + C_4 * WSPD \quad (3)$$

where Tas is the ambient temperature around the cells (°C), RSDS is the downward solar radiation (W m^{-2}), WSPD is the wind speed (m s^{-1}) and C_1, C_2, C_3, and C_4 are coefficients which depend on the PV material properties. From recent studies, it was shown that the wind speed effect on the PVP can be negligible in the West Africa region [20]. We use only the effect of the temperature and the shortwave solar radiation to calculate the Tcell. Equation (3) can be reduced as follows:

$$T_{cell} = C_1 + C_2 * Tas + C_3 * RSDS \quad (4)$$

In this study, we assume that the PVP is generated from a mono-crystalline silicon plant, as they are commonly used in West Africa. For this category of material, the coefficients of Equation (4) are C_1 = 3.75 °C, C_2 = 1.14, and C_3 = 0.0175 °C m^2 W^{-1} based on Crook et al. [12].

2.3.2. Wind Power Density Estimation

The wind power density (WPD) is an important indicator for assessing the potential of wind energy at a site [78]. Following Sawadogo et al. [16], the WPD expressed in W m^{-2} is calculated using the following equation:

$$WPD = \frac{1}{2}\rho(WSPDz)^3 \quad (5)$$

where $WSPD_z$ is the wind speed at 100 m above ground level and the air density ρ. In this study, the 100 m wind speed is calculated by extrapolating the 10 m wind speed, using the power law equation [79]:

$$WSPD_z = WSPD_{zr}\left(\frac{z}{zr}\right)^{\alpha} \quad (6)$$

where z is the turbine hub height (100 m), zr is the reference height (10 m), and $WSPD_{zr}$ is the wind speed at the reference height. We assume that α = 0.143 for open land surfaces [16].

The air density is estimated following Custódio (2009):

$$\rho = \frac{353.4\left(1 - \frac{z}{45271}\right)^{5.2624}}{273.15 + \mathrm{T}} \quad (7)$$

T is the temperature at 100 m height. The calculation is based on a dry adiabatic lapse rate of about 1 °C per 100 m.

2.3.3. RCMs Evaluation and Impact Analysis

The analysis of the CORDEX-CORE ensemble is conducted for a simulation period ranging from 1971 to 2100, from which the period 1971–2000 was taken as reference, 2021–2050 for the near future simulation, and 2071–2100 for the far future and under the RCP8.5 scenario. The RCP8.5 scenario illustrates a somewhat conservative situation of business as usual with low income, high population, and high energy demand. It uses the 90th percentile of the baseline scenario without explicit climate policy and represents the highest RCP scenario in terms of greenhouse gas (GHG) emissions. The choice of this scenario was based on the fact that it is one of the most used emission scenarios in climate projection, which helps to explore an unlikely high-risk future [80,81]. The future period is divided into two time slots: 2021–2050 for the near future and 2071–2100 for the far future. Monthly data are used for all variables calculated from the model and reference datasets. The annual means are obtained by averaging the monthly values and the Mean is obtained by averaging over the three RCMs, which are also averaged over the 3 GCMs. The model evaluation of the RCM is conducted for target variables (Tcell, PVP, and WPD) and further variables (WSPD, Tas, and RSDS) relevant for the calculation of the target variables (Section 2.3) using common performance metrics, such as the root mean square error (RMSE), the mean absolute error (MAE), and the correlation coefficient r using the Equation (8), (9), and (10), respectively.

$$\mathrm{RMSE} = \sqrt{\sum_{i=1}^{n} \frac{(\mathrm{P_i} - \mathrm{O_i})^2}{n}} \quad (8)$$

$$\mathrm{MAE} = \frac{1}{n} \sum_{i=1}^{n} (|\mathrm{P_i} - \mathrm{O_i}|) \quad (9)$$

$$\mathrm{r} = \frac{\sum_{i=1}^{n} (\mathrm{O_i} - \underline{\mathrm{O}})(\mathrm{P_i} - \underline{\mathrm{P}})}{\sqrt{\sum_{i=1}^{n} (\mathrm{O_i} - \underline{\mathrm{O}})^2 \sum_{i=1}^{n} (\mathrm{P_i} - \underline{\mathrm{P}})^2}} \quad (10)$$

where P is the RCM data, O the reference data at timestep i, and n the number of data points. $\underline{\mathrm{O}}$ and $\underline{\mathrm{P}}$ are the mean value of the reference and RMC data, respectively.

The validation of the model output focuses on important climate features (e.g., annual patterns and cycle) in addition to temporal statistics using diagnostic tools such as the Taylor Diagram. Relative to the reference period, the changes in future PVP and WPD over the region are analyzed and no bias adjustments are applied. Indeed, bias requires reference data that reflect the true weather of the location [82]. The reference datasets used in this study are subject to some biases that were pointed out in previous studies [83,84]. A recent study by Dieng et al. [85] showed that the change signals of wind speed and solar irradiance are largely preserved after bias correction over West Africa.

The projected changes in temperature are estimated as the difference between the future and reference periods (absolute change). For the other variables, the changes are estimated in terms of percentage (relative change). A statistical *t*-test is also conducted to indicate the significance of the projected changes at a 95% confidence level. According to Seaby et al. [86], it could be useful to evaluate climate models for statistically significant changes over the 21st century for purposes of model comparison and selection for impact modelling. The *t*-test is among the most common tests used in climate science for the

approximation of the significance of modelled changes [87]. Finally, the model agreement for the projected changes is assessed, as agreement across models became an important tool to evaluate the robustness of model outputs. When multiple independent models agree, their shared conclusion is more likely to be true [88]. In this study, the agreement of the RCMs is designated by the colored areas and the disagreement by uncolored or white areas.

3. Results and Discussion

3.1. Evaluation and Validation of the Model

3.1.1. Annual Patterns of the Climate Variables in the Reference Period

For the validation of the models, a comparison of the model outputs and the reference datasets (ERA5 and SARAH-2) is conducted. Figures 3 and 4 show the simulated and observed spatial patterns of the annual averages for all the variables of this investigation, for the reference period 1971–2000. The RCMs and the ensemble mean show a relatively good representation of the spatial distribution of the different variables. All spatial correlations are greater than 0.8. Despite this performance of the RCMs, there are some pronounced biases. A high bias of PVP and WPD is noticed for all the single RCMs and especially for the Sahel zone. There is a bias ranging from −300 to 150 kWh m^{-2} for PVP and 50 to 150 W m^{-2} for WPD, with CCLM having a strong underestimation of −300 kWh m^{-2} of PVP in the Guinea sub-region. The RCMs present less bias for the other variables. RegCM shows an overestimation of all the climate variables, especially in the Sahel. CCLM presents an underestimation of RSDS over Guinea and Savannah and T_{cell} and Tas over West Africa as a whole. In opposite to RegCM and CCLM, REMO underestimates RSDS and PVP in the Sahel zone but overestimates WSPD and WPD as the other two RCMs. However, the Mean shows a better representation in terms of RMSE, MAE, and correlation, and presents less biases as compared to the single RCMs. Similar biases of RSDS and Tas are shown in the study by Sawadogo et al. [16], who used an ensemble of 14 RCMs from the coordinated regional climate downscaling experiment simulations to investigate the impact of climate change on the production potential of solar PV over West Africa. However, for WSPD, while we find an overestimation of about 2 m s^{-1} over West Africa, results from the studies of Sawadogo et al. [16] and Ogunjobi et al. [17] present a similar overestimation, but only for Guinea and Savannah, and underestimation for the Sahel. Model biases can be related to many factors. These biases could arise from both the driving GCM and the RCM, but differences between the GCMs are usually larger than those between the RCMs, except for coastal areas and regions with complex topography [89]. This study used the CORDEX-CORE datasets, which provide high-resolution regional climate information. Some comparison studies between the global climate models (CMIP5, CMIP6) and regional climate models (CORDEX, CORDEX-CORE) showed a better performance of the CORDEX-CORE in simulating drought and rainfall indices over the region [25,27].

Regardless of these biases, The RCMs are able to reproduce the spatial pattern of the different climate variables. The highest values of RSDS and Tas are in the Sahel zone and the lowest in the Guinea zone. The same observation is indicated for T_{cell} and PVP. This could be explained by a lack of vegetation in the Sahel, a very low amount of precipitation during a short period of time, and a long dry season compared to the Guinea zone, which has a long rainy season. The highest wind speed and wind power density are in the northern coastal area, mainly the northern coast of Senegal, Mauritania, and the Sahel zone. The lowest are in the Guinea zone.

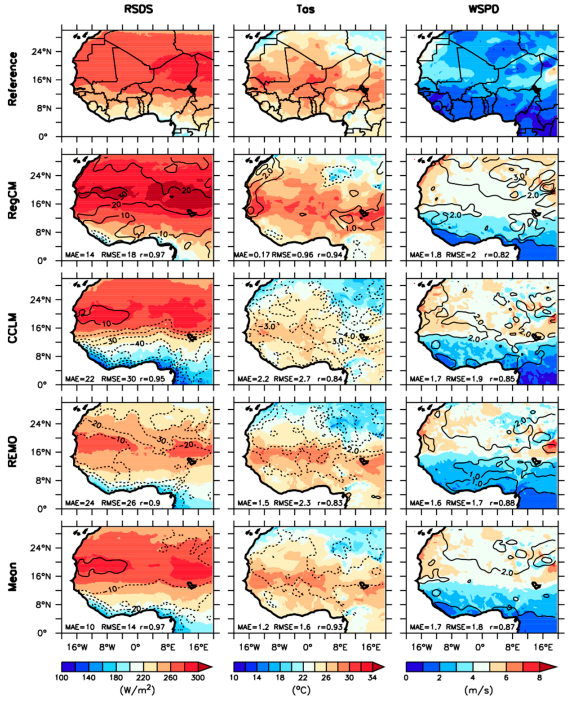

Figure 3. Spatial distribution of the annual averages of observed and simulated solar irradiance (RSDS), ambient air temperature (Tas), and surface wind speed (WSPD) over West Africa. The bias is plotted in contours, and the correlation (r), mean absolute error (MAE), and root mean square error (RMSE) between the observation and the model are also indicated.

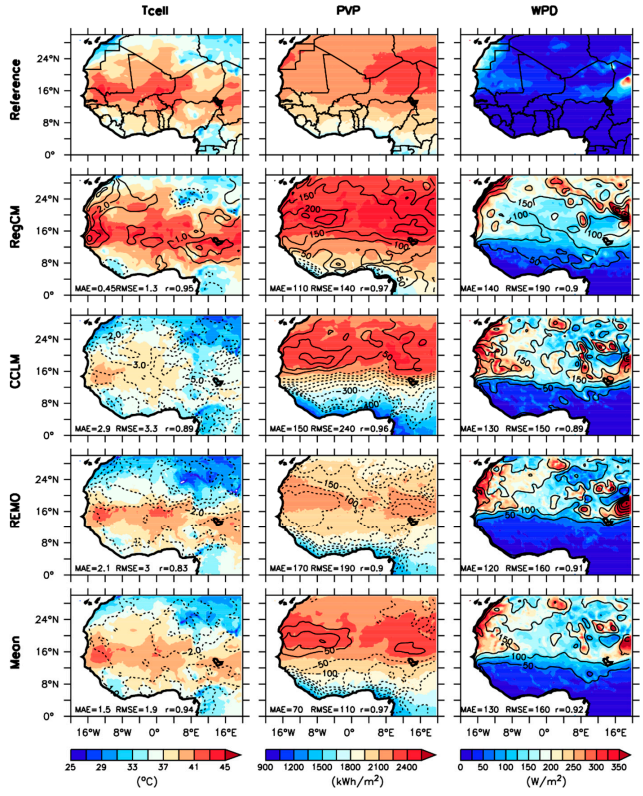

Figure 4. Same as Figure 3, but for cell temperature (T_{cell}), photovoltaic potential (PVP), and wind power density (WPD).

3.1.2. Annual Cycle of the Climate Variables in the Reference Period

For the same variables, the mean annual cycle of the three selected climatic zones of West Africa is represented, namely Sahel, Savannah, and Guinea (Figures 5 and 6). The RCMs capture the pattern of the variables in all regions, although strong overestimations are present, especially for the wind variables. Comparing the model's performance, the temperature variables (Tas and T_{cell}) are better simulated by the RCMs, which capture not only the pattern, but also the amplitude in the three areas of the region, apart from a slight underestimation of the CCLM model.

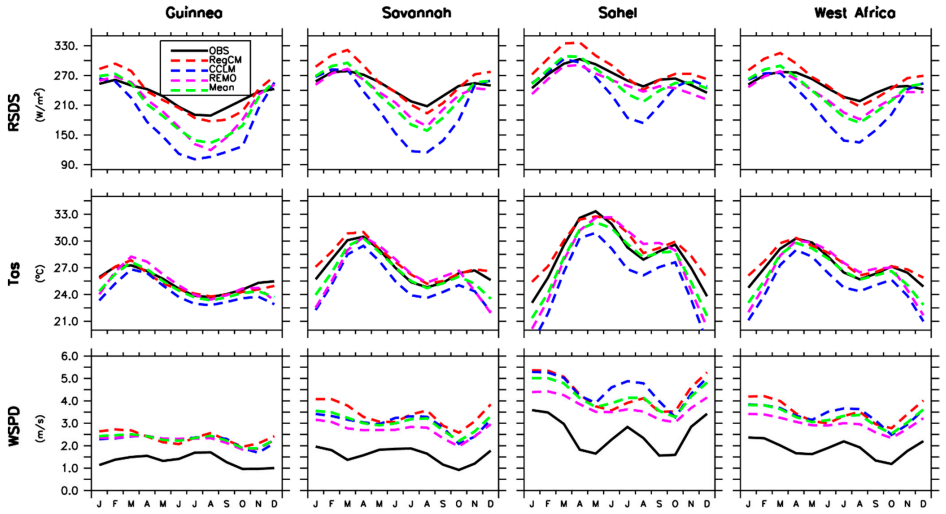

Figure 5. Annual cycle of observed and simulated solar irradiance (RSDS), ambient air temperature (Tas), and surface wind speed (WSPD) over the three climatic zones of West Africa.

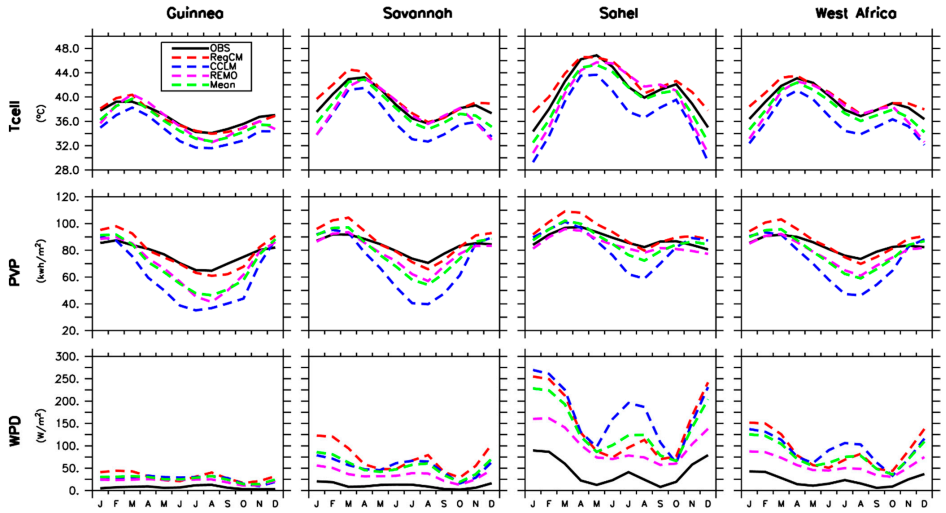

Figure 6. Annual cycle of observed and simulated cell temperature (Tcell), solar, and wind potential (PVP and WPD, respectively) over the three climatic zones of West Africa.

The WSPD and the WPD are strongly overestimated by all the RCMs and the Mean as well as in all climatic zones with higher biases observed for the WSPD than the WPD and the Sahel zone. Nevertheless, the RCMs agree well with the pattern of these variables, with REMO showing better amplitudes and less bias compared to the other RCMs. The highest values of WSPD and WPD are in the Sahel with two peaks in February and in July, with WSPD reaching almost 4 m-s^{-1} in the Harmattan period (DJF). RSDS and PVP exhibit the same pattern according to the region. The RCMs and the Mean underestimate the RSDS

and PVP from March to November, with RegCM presenting a better representation in the different areas.

3.1.3. Model Performance in the Reference Period

To evaluate the accuracy and other quality attributes (e.g., correlation and standard deviation) of the model simulations, a statistical analysis is also performed using a Taylor diagram (Figure 7). The Taylor diagram is an analysis of the monthly average of the variables over each climatic zone. The black dot indicates data perfect model simulation, while the other colored dots indicate that of the different RCMs simulations. The Mean and RegCM perform best in most cases for the radiation variables (RSDS and PVP) with better results for Guinea and Savannah compared to the Sahel zone. CCLM is the least efficient model for RSDS and PVP simulations. In the case of the wind variables, REMO is the best model among the RCMs for representing WSPD and WPD in the sub-regions and West Africa, therefore confirming the findings of the previous section. The simulations of T_{cell} and Tas present smaller differences in the normalized standard deviation for the RCMs than the wind and radiation variables. CCLM shows better performance in the Tas and T_{cell} simulations. Nevertheless, there is more consistency between the observation and simulation in the other zones than in the Sahel.

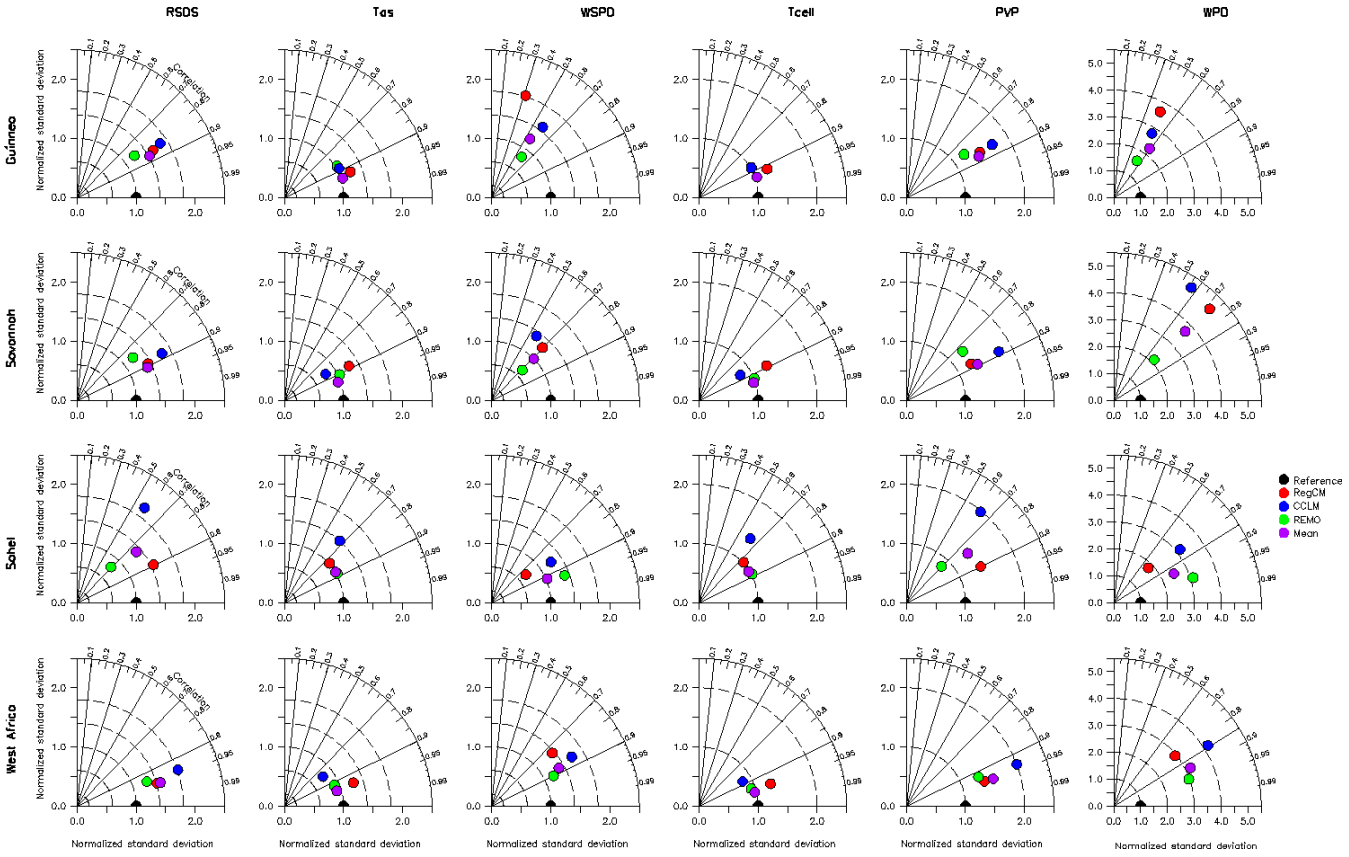

Figure 7. Taylor diagram of the observed and simulated solar irradiance (RSDS), ambient air temperature (Tas), surface wind speed (WSPD), cell temperature (T_{cell}), photovoltaic potential (PVP), and wind power density (WPD) in the reference period and over the three sub-regions of West Africa.

Basically, the models show a high disparity for the WSPD and WPD simulations and for all the sub-regions. The same disparities in the simulation of all the climate variables and for the Sahel zone are noticed. Across the individual RCMs and the individual climate variables, the model RegCM is the best at simulating the RSDS and PVP in the sub-regions. For the WSPD and WPD simulations, REMO best fits the observation in the different zones. Both REMO and RegCM perform well in the simulations of the temperature variables.

3.2. Projected Climate Changes

3.2.1. Future Temperature, Shortwave Solar Radiation, and Wind Speed Changes

All three RCMs agree that there will be significant warming over West Africa (Figures 8 and 9). This increase in temperature is more pronounced in the far future than in the near future. However, the magnitude of the changes varies according to the RCM in both periods. For instance, where RegCM, REMO, and Mean project an increase of around 2.5 to 3 °C, CCLM projects lower temperatures (~2 °C) for the northern coast of Senegal and around Mauritania. For the near future, the highest temperatures are above 16 °N for RegCM, while for REMO, they are in the northern part of Mali and Niger. The Mean shows an increase of 2.5 °C over the Savannah and Sahel zones, while in Guinea, it projects lower values of around 1.5 °C. This uncertainty in the degree of warming is also discussed by Deme et al. [90] who found differences in the warming trend in the north of 15° N (where 3.5 °C is reached) and south of 15° N (2 °C) over the period 2041–2070 with more moderate warming across the Guinean coast under the RCP8.5 scenario.

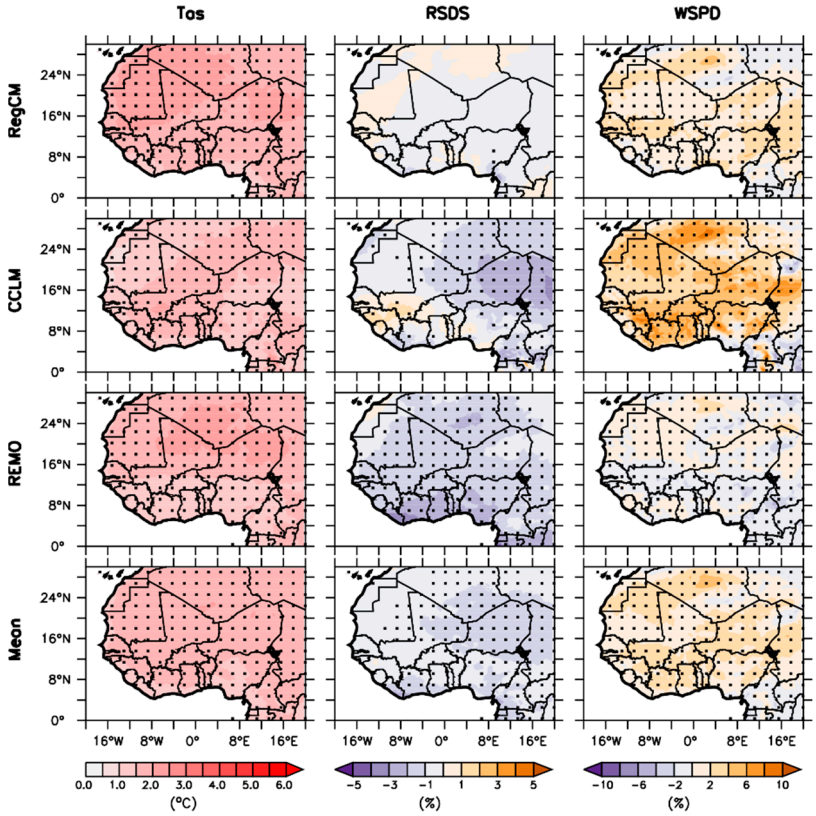

Figure 8. Projected changes in the annual average of solar irradiance (RSDS), ambient air temperature (Tas), and surface wind speed (WSPD) over West Africa for the near future (2021–2050) and under the RCP8.5 scenario. Statistically significant areas are indicated with black dots.

In contrast, to the temperature projection, a much more diverse picture is shown for RSDS and WSPD projections. A general decrease in RSDS is projected by RegCM, REMO, and Mean for the near and far future. For the near future, RegCM projects a slight decrease (−1%), which is not significant in most parts of the region, and a slight increase (~1%) over Senegal and Mauritania. For the far future, a significant decrease is projected in Niger, Mali, and the Guinea zone (~−3%). The REMO model indicates a significant decrease in almost all West African countries for both periods. A decrease of ~−3% and ~−2% for the Guinea and Sahel areas, respectively, in the near future, and ~−5% and ~−3% in the far future. These results are consistent with those of Huber et al. [18], who projected that solar irradiance is likely to decrease mainly in southern and western Africa. In addition, Sawadogo et al. [16] projected a general decrease in RSDS over West Africa. Only CCLM

projected a significant increase (~2%) over Savannah and a significant decrease (~3%) over northern Mali and Niger, for the near future. A significant increase of up to 5% is projected over Guinea, Savannah, and Sahel for the far future.

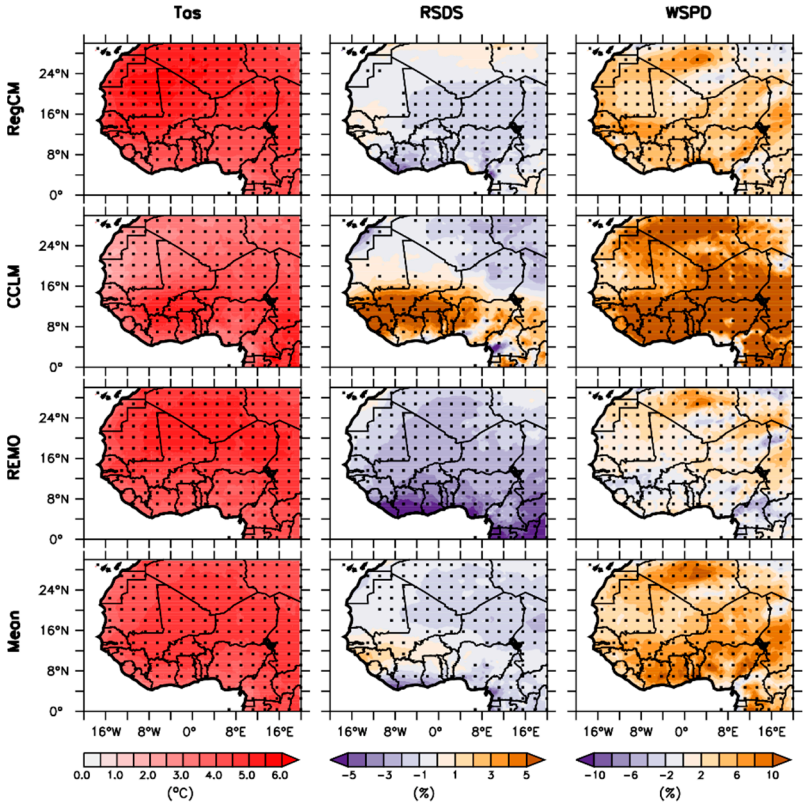

Figure 9. Same as Figure 8 but for the far future (2071–2100) and under the RCP8.5 scenario.

The projected decrease in RSDS could be explained by an increase in aerosol and cloud cover. Future changes in these parameters will be directly linked to the projected changes in surface irradiance [21]. In their study, Danso et al. [21] investigated the relationship between the change in surface irradiance, the cloud water path (CWP) and the aerosol optical depth (AOD) at 550 nm, using multiple linear regression. The results show negative coefficients between CWP and AOD changes and the surface irradiance. They conclude that a unit increase in either CWP or AOD will result in a decrease in surface irradiance.

There are also discrepancies between the models in the wind speed projection. In both future periods, RegCM, CCLM, and Mean show a dominant increase in WSPD (up to 10% for the far future) which is also statistically significant over the region, whereas REMO shows a decrease in most parts of the region and for both periods.

3.2.2. Changes in Cell Temperature, PV Potential and Wind Power Density

The projection of these variables is similar to that of Tas, RSDS, and WSPD. The formulae presented in Section 2.3 show the dependence of the variables. As noted in the previous section on Tas, the projection of T_{cell} shows an increase across the region, which is higher and more accentuated in the far future. In the near future, the lower values of T_{cell} are in the Guinea zone for RegCM, REMO, and Mean (~2 °C), while for CCLM, they are on the northern coast of Senegal and around Mauritania. In the far future, a general increase of about 4 °C to 6 °C is projected by the RCMs and Mean. As shown in Equation (4), T_{cell} depends only on air temperature and solar radiation. Since the radiation changes are marginal, the increase in T_{cell} may be due to the relatively strong increase in air temperature.

A general decrease in PVP is projected over the region (Figures 10 and 11). The Mean shows a decrease of −2% in the near future and more than −3% in the far future. All RCMs agree on the magnitude of the changes in the far future (>−2.4%) except CCLM, which projects lower values ranging between −0.8 and −1.6% in the north of Senegal, Mali, Mauritania, north of Niger, and Algeria. The RegCM model indicates that the Sahel area will experience a higher decrease in PVP than the Guinea and Savannah areas in the near future, while REMO projects a higher decrease in the north of Mali, Niger, and a part of Algeria. The spatial variation in PVP in the region could be explained by the spatial variation in T_{cell} and RSDS. The PVP is sensitive to Tcell, which can induce its reduction. According to Mavromatakis et al. [71], one of the main factors causing the power output of a PV system to decrease is the increase in its temperature. Another factor is solar irradiance since it is the dominant variable for PVP calculation. For instance, Sawadogo et al. [16] found a strong positive correlation between RSDS and PVP ($r > 0.93$). The decrease in PVP in West Africa was shown by several studies [16,18,19,21]. As shown in the previous section, RCM simulations suffer from biases and other limitations, but the future decrease in the PVP over West Africa seems evident even though the magnitude of the decrease varies among the RCMs.

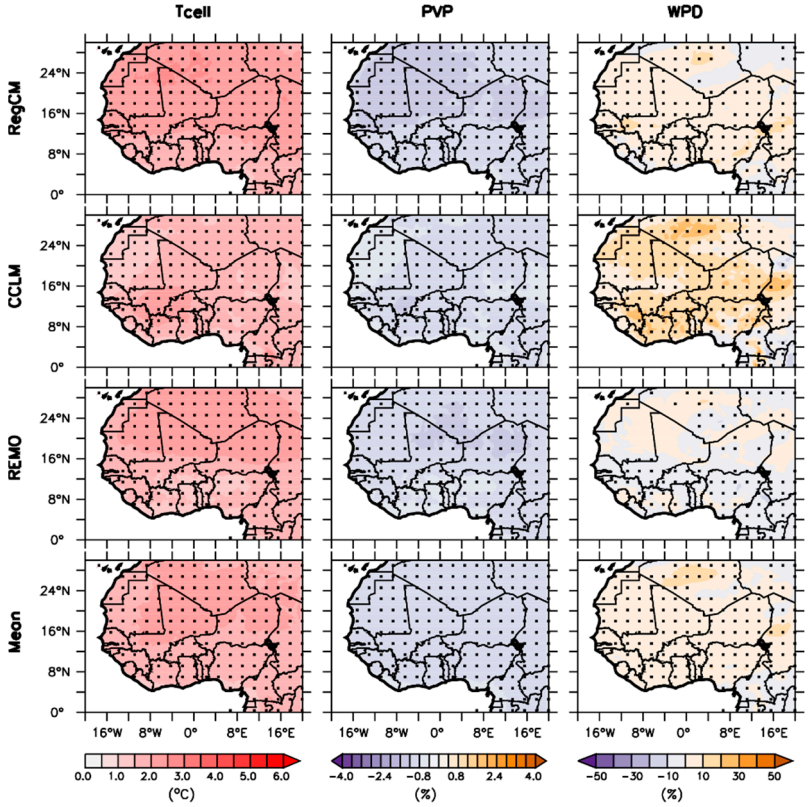

Figure 10. Projected changes in the annual average of the cell temperature (Tcell), photovoltaic potential (PVP), and wind power density (WPD) over West Africa for the near future (2021–2050) and under the RCP8.5 scenario. Statistically significant areas are indicated with black dots.

Conversely, the projection of WPD is subject to some uncertainties (Figures 10 and 11). The models RegCM and CCLM, as well as the Mean, project a dominant increase of up to 20% in near future, but more pronounced in the far future (~40%). REMO is more likely to project a dominant decrease of about −10% in most parts of the region in both future scenarios. The results of the studies of wind power potential in West Africa are quite diverse. The uncertainties in the projection of wind energy potential are larger than those of solar PV potential over West Africa. This could be due to the consistency of the models in simulating the temperature and solar radiation compared to the representation of the wind speed.

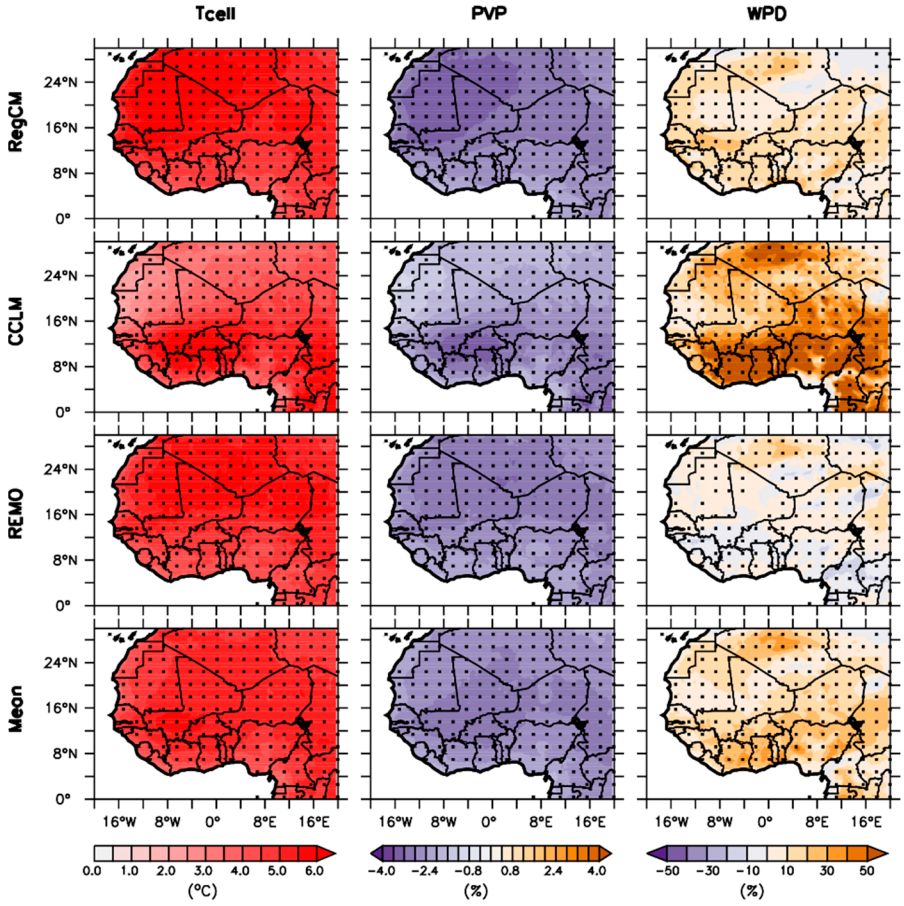

Figure 11. Same as Figure 10, but for the far future (2071–2100) and under the RCP8.5 scenario.

The results of this study are in line with those of Sawadogo et al. [14], who projected an increase in the WPD when using the RegCM4 CORDEX-CORE ensemble. However, they are in contradiction with the study of Ogunjobi et al. [17], who found a decline in the wind production in Guinea and Savannah in the near future (2021–2050) before increasing towards the end of the century under RCP4.5 and RCP8.5 scenarios. It is noted that results obtained at lower resolution (CORDEX, CMIP6) show a decrease in wind power density over the Sahel Akinsanola et al. [91] and over Guinea and Savannah Ogunjobi et al. [17], where an increase is projected in our study.

3.3. Inter-Annual Variability

Figure 12 shows the inter-annual variability of Tcell, PVP, and WPD under the RCP8.5 scenario and for the mid and late centuries. The models broadly agree on the pattern and magnitude of Tcell and PVP projections as compared to WPD in all the sub-regions. For both future scenarios, the RCMs indicate a progressive increment in Tcell and a decrease in PVP. In the near future, for all sub-regions, a rapid increase in Tcell of about 3 °C for the Sahel and Savannah, 2.4 °C for Guinea, and about 2.7 °C for West Africa were found for the period 2021–2050, and about 6 °C and 5 °C for Sahel-Savannah and Guinea, respectively, by the end of the century. For the same period of 2021–2050, the decrease in PVP is slightly stronger (−2%) in the Sahel-Savannah than in Guinea, (~−1.4%) and becomes more pronounced in the far future where the values for Sahel-Savannah and Guinea reach −3.5% and −3%, respectively.

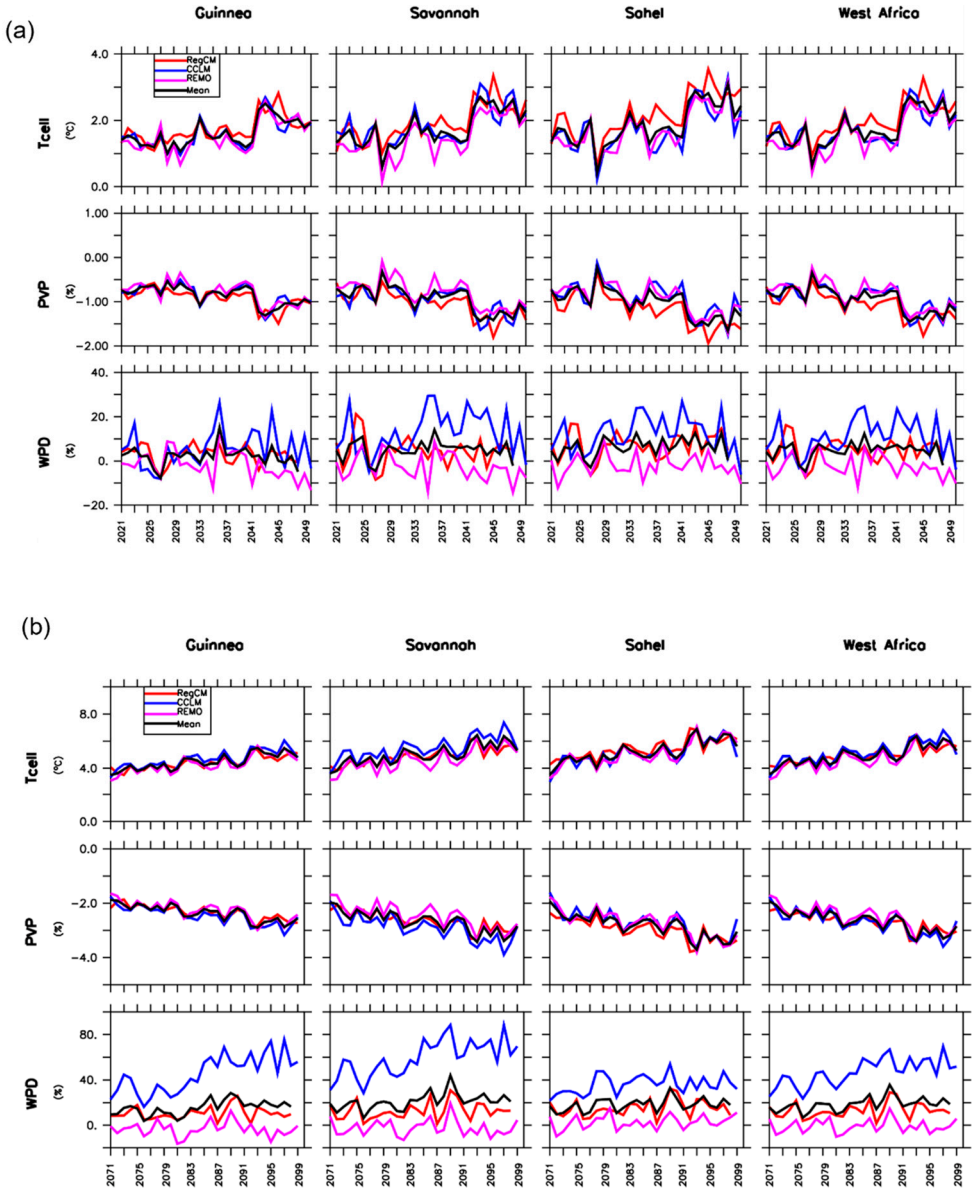

Figure 12. Inter-annual variability of the projected changes of the cell temperature (Tcell) and the solar and wind potential (PVP and WPD respectively) over the climatic zones of West Africa for the near future (**a**) (2021–2050) and far future (**b**) (2071–2100) and under the RCP8.5 scenario.

The inter-annual variability of WPD shows a divergence between the models. CCLM predicts a higher magnitude in the projected WPD in both periods and for all the climatic zones. In the mid-century, CCLM and REMO project a slight increase and a slight decrease in WPD over the region, respectively. In comparison, CCLM expects a sharp increase for the period of 2071–2100, which in terms of intensity at the end of the century, is about 60% for the Guinea zone, about 65% for the Savannah, and 40% for the Sahel. On the other hand, REMO expects a slight decrease in WPD of about −3 to 5% for Guinea, Savannah, and the whole region of West Africa and no major change for the Sahel. RegCM and Mean tend to show no major variations in the near future and an increase between 10 and 20% in the far future.

3.4. Models' Agreement on the Projected Changes

The representation of the agreement between the models for the projections of the variables (Figure 13) shows a general agreement across the region for Tas (near and far future) and Tcell (near future). This shows a robust projected change for the temperature

variables. The RCMs agree on warming and project a 1 °C increase in the air temperature in the near future and between 3.5 °C and 4 °C in the far future with Mali, Burkina, and Niger experiencing the highest temperatures at the end of the century. The models also expect an increase in Tcell of 1 °C to 1.5 °C in the near future. In the far future, an increment of 3.5 °C to 5 °C is expected in the northern part of the region, mainly the Sahel zone, in some parts of Savannah and above 16° N. This is also valid for the other variables, such as WSPD, PVP, and WPD, where the RCMs show consistent agreement results in the same zones.

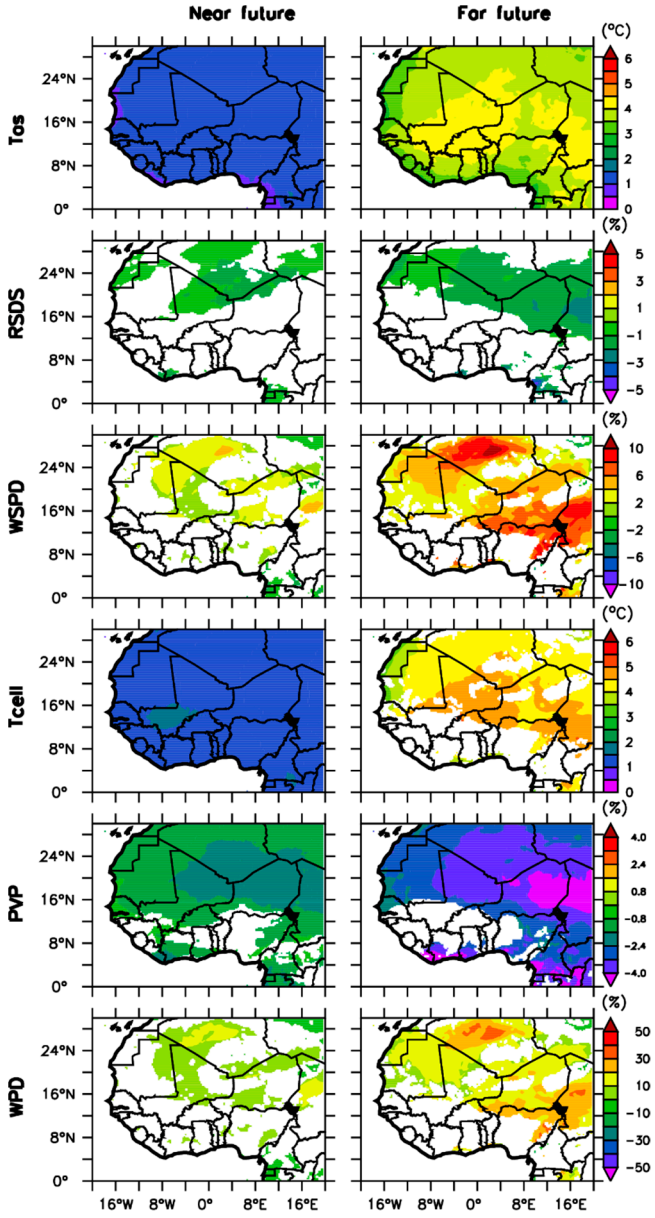

Figure 13. Models agreement: Projected changes in the annual average of solar irradiance (RSDS), temperature (Tas), surface wind speed (WSPD), cell temperature (Tcell), photovoltaic potential (PVP), and wind power density (WPD) over West Africa for the near (2021–2050) and far future (2071–2100) under the RCP8.5 scenario. The white color indicates areas where the models disagree.

For the decrease in PVP, the models disagree in most parts of Guinea and Savannah, as well as for both future periods. A general decrease ranges between −0.8 and −2.4%, and more than −2.4% over the Sahel area and above 16° N, respectively, in the near and far future is projected. A similar agreement is noticed for WSPD and WPD for both periods. Unlike PVP, the disagreement in WPD is spread over the region in both periods, it is not

just limited to one area. The RCMs agree majorly in Niger, the north of Mali, and Nigeria, but also around Mauritania and Algeria, for the far future. In these areas, an increase in WPD ranges between 10 and 20% is expected. The projection of the temperature variables and PVP show more consistent agreement as compared to RSDS, WSPD, and WPD. In summary, most parameters show inconsistency in the sign of future changes in some areas, which could be related to the internal variability of the model, the initial conditions, or the configurations of the different GCMs [92]. A lack of agreement and therefore implies lower reliability of projected change in these variables over the considered period.

4. Summary and Conclusions

This study presents the projected changes in solar PV and wind energy potential over West Africa using CORDEX-CORE ensemble simulations. Three regional climate models (RCMs), driven by three different GCMs, namely NorESM1-M, MPI-ESM-MR, and HadGEM2-ES from the CMIP5, were used. The expected changes in solar PV and wind potential, as well as related variables such as air temperature, solar radiation, and wind speed, were analyzed. The results of our investigation can be summarized as follows:

- The model evaluation shows a relatively good representation of selected annual and monthly patterns of the simulated solar PV potential, the wind power density, and related variables, with high spatial correlations ranging between 0.82 and 0.97. However, we also identified strong under and overestimations of the RCM simulations, especially for the wind variables.
- RegCM is the best model among the RCMs for the simulations of the solar irradiance and the solar PV potential and the sub-regions.
- REMO is the best model for wind speed and wind power density simulation over the region.
- For the air temperature, both REMO and RegCM had a good performance. CCLM was the least efficient model for this simulation.
- A better simulation of these variables with less biases is noted when using the ensemble mean.
- The projection under the RCP8.5 scenario indicates a decrease in solar irradiance and solar PV potential. The solar PV potential is expected to have a significant decrease for all the RCMs and the ensemble mean, as well as for the near (2021–2051) and far future (2071–2100), and under the RCP8.5 scenario. The decrease concerns the whole of West Africa and varies from ~−2 to about −4% in the considered period. This is mainly due to the increase in cell temperature and the decrease in solar radiation over the region.
- The wind power projection shows a predominant increase over West Africa, with a projection of about 20 to 40% by the ensemble mean and for the two future periods. The RCMs convey more consistency in the projection of the other climate variables than the wind speed and the wind power density. The latter is subject to some divergences, with REMO expecting a decrease, RegCM and Mean an increase, and CCLM a high increase.

The CORDEX-CORE provides, in a consistent manner, a high-resolution dataset of RCM projections for West Africa. However, the current projections are only based on three RCMs, as they are the only modelling groups that participated in the CORE initiative (to date). Therefore, a relatively small ensemble of RCM projections is used to determine the inherent uncertainty of climate projections. To reduce the uncertainties in the climate projections, more simulations should be available from the CORDEX-CORE, similar to the CORDEX data (~50 km). Another limitation of this work is that we only consider the RCP8.5 scenario. The results of this study could be improved by considering other scenarios like the RCP2.6 and 4.5 scenarios. Future studies could also assess the robustness of the projected change in wind and solar energy from CORDEX-CORE over the West Africa region. Nevertheless, the study shows useful results, which are an important contribution to research on the future changes in solar PV and wind energy potential over West Africa. The results of this study can help governments and policymakers in targeting RES for

future projects as part of the energy transition for climate change mitigation by considering the impacts of climate change on these resources.

Author Contributions: Conceptualization, A.N.; Methodology, A.N., W.S.; Software, A.N.; Formal analysis, A.N., J.B., C.D., M.S.M.; Writing—original draft, A.N.; Writing—review & editing, A.N., M.S.M., C.D., W.S., J.B., L.D. and H.K.; Supervision, M.S.M., C.D., J.B., L.D. and H.K. All authors have read and agreed to the published version of the manuscript.

Funding: This publication was produced with the financial support of the German Ministry for Education and Research (BMBF) through the West African Science Service Center on Climate Change and Adapted Land Use (WASCAL) and the Prince Albert II of Monaco Foundation. The contents of this document are solely the liability of Aissatou Ndiaye and under no circumstances may be considered as a reflection of the position of the Prince Albert II of Monaco Foundation and/or the IPCC. The work was also done as a part of the ENERSHELF (Grant number: 03SF0567D) project funded by the BMBF.

Data Availability Statement: The data presented in this study are openly available at https://cordex.org/data-access/esgf/ (1 October 2022); https://www.ecmwf.int//en/forecasts/datasets/reanalysis-datasets/era5 (1 October 2022); https://wui.cmsaf.eu/safira/action/viewDoiDetails?acronym=SARAH_V002_0 (1 October 2022).

Acknowledgments: The authors acknowledge the World Climate Research Program's Working Group for access to the CORDEX-CORE datasets. We also thank ECMWF and SARAH-2 for access to their datasets used in this study.

Conflicts of Interest: The authors declare no conflict of interest.

References

1. U.S. Energy Information Administration. International Energy Outlook 2019. 2019. Available online: www.eia.gov/ieo (accessed on 2 March 2022).
2. Foster and Elzing, United Nation Website, December 2015. Available online: https://www.un.org/en/chronicle/article/role-fossil-fuels-sustainable-energy-system (accessed on 2 March 2022).
3. Eyring, V.; Gillett, N.P.; Rao, K.M.A.; Barimalala, R.; Parrillo, M.B.; Bellouin, N.; Cassou, C.; Durack, P.J.; Kosaka, Y.; McGregor, S.; et al. Human Influence on the Climate System. In *Climate Change 2021: The Physical Science Basis. Contribution of Working Group I to the Sixth Assessment Report of the Intergovernmental Panel on Climate Change*; Cambridge University Press: Cambridge, UK, 2021; pp. 423–552. [CrossRef]
4. Moomaw, W.; Yamba, F.; Kamimoto, M.; Maurice, L.; Nyboer, J.; Urama, K.; Weir, T.; Bruckner, T.; Jäger-Waldau, A.; Krey, V.; et al. Renewable Energy and Climate Change. In *IPCC Special Report on Renewable Energy Sources and Climate Change Mitigation*; Cambridge University Press: Cambridge, UK, 2011; pp. 161–208. [CrossRef]
5. International Energy Agency. Renewables. 2019. Available online: www.iea.org/renewables2019 (accessed on 4 March 2022).
6. Chandramowli, S.; Felder, F.A. Impact of climate change on electricity systems and markets – A review of models and forecasts. *Sustain. Energy Technol. Assess.* **2014**, *5*, 62–74. [CrossRef]
7. Troccoli, A.; Goodess, C.; Jones, P.; Penny, L.; Dorling, S.; Harpham, C.; Dubus, L.; Parey, S.; Claudel, S.; Khong, D.-H.; et al. Creating a proof-of-concept climate service to assess future renewable energy mixes in Europe: An overview of the C3S ECEM project. *Adv. Sci. Res.* **2018**, *15*, 191–205. [CrossRef]
8. Pryor, S.; Barthelmie, R. Climate change impacts on wind energy: A review. *Renew. Sustain. Energy Rev.* **2010**, *14*, 430–437. [CrossRef]
9. Tobin, I.; Vautard, R.; Balog, I.; Bréon, F.-M.; Jerez, S.; Ruti, P.M.; Thais, F.; Vrac, M.; Yiou, P. Assessing climate change impacts on European wind energy from ENSEMBLES high-resolution climate projections. *Clim. Change* **2014**, *128*, 99–112. [CrossRef]
10. Müller, J.; Folini, D.; Wild, M.; Pfenninger, S. CMIP-5 models project photovoltaics are a no-regrets investment in Europe irrespective of climate change. *Energy* **2018**, *171*, 135–148. [CrossRef]
11. Breslow, P.B.; Sailor, D.J. Vulnerability of wind power resources to climate change in the continental United States. *Renew. Energy* **2002**, *27*, 585–598. [CrossRef]
12. Crook, J.A.; Jones, L.A.; Forster, P.M.; Crook, R. Climate change impacts on future photovoltaic and concentrated solar power energy output. *Energy Environ. Sci.* **2011**, *4*, 3101–3109. [CrossRef]
13. De Jong, P.; Barreto, T.B.; Tanajura, C.A.; Kouloukoui, D.; Oliveira-Esquerre, K.P.; Kiperstok, A.; Torres, E.A. Estimating the impact of climate change on wind and solar energy in Brazil using a South American regional climate model. *Renew. Energy* **2019**, *141*, 390–401. [CrossRef]
14. Sawadogo, W.; Abiodun, B.J.; Okogbue, E.C. Impacts of global warming on photovoltaic power generation over West Africa. *Renew. Energy* **2019**, *151*, 263–277. [CrossRef]

15. Soares, P.M.M.; Lima, D.C.; Semedo, A.; Cabos, W.; Sein, D.V. Climate change impact on Northwestern African offshore wind energy resources. *Environ. Res. Lett.* **2019**, *14*, 124065. [CrossRef]
16. Sawadogo, W.; Abiodun, B.J.; Okogbue, E.C. Projected changes in wind energy potential over West Africa under the global warming of 1.5 °C and above. *Theor. Appl. Clim.* **2019**, *138*, 321–333. [CrossRef]
17. Ogunjobi, K.O.; Ajayi, V.O.; Folorunsho, A.H.; Ilori, O.W. Projected changes in wind energy potential using CORDEX ensemble simulation over West Africa. *Arch. Meteorol. Geophys. Bioclimatol. Ser. B* **2022**, *134*, 48. [CrossRef]
18. Huber, I.; Bugliaro, L.; Ponater, M.; Garny, H.; Emde, C.; Mayer, B. Do climate models project changes in solar resources? *Sol. Energy* **2016**, *129*, 65–84. [CrossRef]
19. Bazyomo, S.D.Y.B.; Lawin, E.A.; Coulibaly, O.; Ouedraogo, A. Forecasted Changes in West Africa Photovoltaic Energy Output by 2045. *Climate* **2016**, *4*, 53. [CrossRef]
20. Sawadogo, W.; Reboita, M.S.; Faye, A.; Da Rocha, R.P.; Odoulami, R.C.; Olusegun, C.F.; Adeniyi, M.O.; Abiodun, B.J.; Sylla, M.B.; Diallo, I.; et al. Current and future potential of solar and wind energy over Africa using the RegCM4 CORDEX-CORE ensemble. *Clim. Dyn.* **2021**, *57*, 1647–1672. [CrossRef]
21. Danso, D.K.; Anquetin, S.; Diedhiou, A.; Lavaysse, C.; Hingray, B.; Raynaud, D.; Kobea, A.T. A CMIP6 assessment of the potential climate change impacts on solar photovoltaic energy and its atmospheric drivers in West Africa. *Environ. Res. Lett.* **2022**, *17*, 044016. [CrossRef]
22. Gutowski, J.W.; Giorgi, F.; Timbal, B.; Frigon, A.; Jacob, D.; Kang, H.S.; Raghavan, K.; Lee, B.; Lennard, C.; Nikulin, G.; et al. WCRP COordinated Regional Downscaling EXperiment (CORDEX): A diagnostic MIP for CMIP6. *Geosci. Model. Dev.* **2016**, *9*, 4087–4095. [CrossRef]
23. Giorgi, F.; Coppola, E.; Teichmann, C.; Jacob, D. Editorial for the CORDEX-CORE Experiment I Special Issue. *Clim. Dyn.* **2021**, *57*, 1265–1268. [CrossRef]
24. Olusegun, C.F.; Awe, O.; Ijila, I.; Ajanaku, O.; Ogunjo, S. Evaluation of dry and wet spell events over West Africa using CORDEX-CORE regional climate models. *Model. Earth Syst. Environ.* **2022**, *8*, 4923–4937. [CrossRef]
25. Dosio, A.; Jury, M.W.; Almazroui, M.; Ashfaq, M.; Diallo, I.; Engelbrecht, F.A.; Klutse, N.A.B.; Lennard, C.; Pinto, I.; Sylla, M.B.; et al. Projected future daily characteristics of African precipitation based on global (CMIP5, CMIP6) and regional (CORDEX, CORDEX-CORE) climate models. *Clim. Dyn.* **2021**, *57*, 3135–3158. [CrossRef]
26. Torres-Alavez, J.A.; Das, S.; Corrales-Suastegui, A.; Coppola, E.; Giorgi, F.; Raffaele, F.; Bukovsky, M.S.; Ashfaq, M.; Salinas, J.A.; Sines, T. Future projections in the climatology of global low-level jets from CORDEX-CORE simulations. *Clim. Dyn.* **2021**, *57*, 1551–1569. [CrossRef]
27. Coppola, E.; Raffaele, F.; Giorgi, F.; Giuliani, G.; Gao, X.; Ciarlo, J.M.; Sines, T.R.; Torres-Alavez, J.A.; Das, S.; di Sante, F.; et al. Climate hazard indices projections based on CORDEX-CORE, CMIP5 and CMIP6 ensemble. *Clim. Dyn.* **2021**, *57*, 1293–1383. [CrossRef]
28. Tebaldi, C.; Knutti, R. The use of the multi-model ensemble in probabilistic climate projections. *Philos. Trans. R. Soc. A Math. Phys. Eng. Sci.* **2007**, *365*, 2053–2075. [CrossRef] [PubMed]
29. Renewable Energy Agency. Unleashing the Solar Potential in ECOWAS: Seeking Areas of Opportunity for Grid-Connected and Decentralised PV Applications. An Opportunity-Based Approach about IRENA. 2013. Available online: www.irena.org (accessed on 7 March 2022).
30. Nicholson, S.E. The West African Sahel: A Review of Recent Studies on the Rainfall Regime and Its Interannual Variability. *ISRN Meteorol.* **2013**, *2013*, 453521. [CrossRef]
31. Lewis, K.; Buontempo, C. *Climate Impacts in the Sahel and West Africa: The Role of Climate Science in Policy Making*; West African Papers, No. 02; OECD Publishing: Paris, France, 2016. [CrossRef]
32. Abiodun, B.J.; Adeyewa, Z.D.; Oguntunde, P.; Salami, A.; Ajayi, V.O. Modeling the impacts of reforestation on future climate in West Africa. *Arch. Meteorol. Geophys. Bioclimatol. Ser. B* **2012**, *110*, 77–96. [CrossRef]
33. Heinzeller, D.; Dieng, D.; Smiatek, G.; Olusegun, C.; Klein, C.; Hamann, I.; Salack, S.; Bliefernicht, J.; Kunstmann, H. The WASCAL high-resolution regional climate simulation ensemble for West Africa: Concept, dissemination and assessment. *Earth Syst. Sci. Data* **2018**, *10*, 815–835. [CrossRef]
34. Dieng, D.; Laux, P.; Smiatek, G.; Heinzeller, D.; Bliefernicht, J.; Sarr, A.; Gaye, A.T.; Kunstmann, H. Performance Analysis and Projected Changes of Agroclimatological Indices Across West Africa Based on High-Resolution Regional Climate Model Simulations. *J. Geophys. Res. Atmos.* **2018**, *123*, 7950–7973. [CrossRef]
35. Akinsanola, A.A.; Ogunjobi, K.O.; Gbode, I.E.; Ajayi, V.O. Assessing the Capabilities of Three Regional Climate Models over CORDEX Africa in Simulating West African Summer Monsoon Precipitation. *Adv. Meteorol.* **2015**, *2015*, 1–13. [CrossRef]
36. Biasutti, M. Rainfall trends in the African Sahel: Characteristics, processes, and causes. *WIREs Clim. Change* **2019**, *10*, e591. [CrossRef]
37. Hersbach, H.; Bell, B.; Berrisford, P.; Hirahara, S.; Horanyi, A.; Muñoz-Sabater, J.; Nicolas, J.; Peubey, C.; Radu, R.; Schepers, D.; et al. The ERA5 global reanalysis. *Q. J. R. Meteorol. Soc.* **2020**, *146*, 1999–2049. [CrossRef]
38. Pfeifroth, U.; Kothe, S.; Müller, R.; Trentmann, J.; Hollmann, R.; Fuchs, P.; Werscheck, M. *Surface Radiation Data Set—Heliosat (SARAH)—Edition 2 (Version 2.0) [Data Set]*; Satellite Application Facility on Climate Monitoring (CM SAF): Deutscher, Germany, 2017. [CrossRef]

39. Taylor, K.E.; Stouffer, R.J.; Meehl, G.A. An Overview of CMIP5 and the Experiment Design. *Bull. Am. Meteorol. Soc.* **2012**, *93*, 485–498. [CrossRef]
40. Giorgi, F.; Coppola, E.; Jacob, D.; Teichmann, C.; Omar, S.A.; Ashfaq, M.; Ban, N.; Bülow, K.; Bukovsky, M.; Buntemeyer, L.; et al. The CORDEX-CORE EXP-I Initiative: Description and Highlight Results from the Initial Analysis. *Bull. Am. Meteorol. Soc.* **2022**, *103*, E293–E310. [CrossRef]
41. Giorgi, F.; Coppola, E.; Solmon, F.; Mariotti, L.; Sylla, M.B.; Bi, X.; Elguindi, N.; Diro, G.T.; Nair, V.; Giuliani, G.; et al. RegCM4: Model description and preliminary tests over multiple CORDEX domains. *Clim. Res.* **2012**, *52*, 7–29. [CrossRef]
42. Elguindi, N.; Turuncoglu, U.; Giorgi, F. Assessment of CMIP5 global model simulations over the sub-set of CORDEX domains used in the Phase I CREMA. *Clim. Change* **2013**, *125*, 3121.
43. McSweeney, C.F.; Jones, R.G.; Lee, R.W.; Rowell, D.P. Selecting CMIP5 GCMs for downscaling over multiple regions. *Clim. Dyn.* **2015**, *44*, 3237–3260. [CrossRef]
44. Jacob, D.; Elizalde, A.; Haensler, A.; Hagemann, S.; Kumar, P.; Podzun, R.; Rechid, D.; Remedio, A.R.; Saeed, F.; Sieck, K.; et al. Assessing the Transferability of the Regional Climate Model REMO to Different COordinated Regional Climate Downscaling EXperiment (CORDEX) Regions. *Atmosphere* **2012**, *3*, 181–199. [CrossRef]
45. Remedio, A.R.; Teichmann, C.; Buntemeyer, L.; Sieck, K.; Weber, T.; Rechid, D.; Hoffmann, P.; Nam, C.; Kotova, L.; Jacob, D. Evaluation of New CORDEX Simulations Using an Updated Köppen–Trewartha Climate Classification. *Atmosphere* **2019**, *10*, 726. [CrossRef]
46. Kouassi, A.A.; Kone, B.; Silue, S.; Dajuma, A.; N'Datchoh, T.E.; Adon, M.; Yoboue, V.; Diedhiou, A. Sensitivity Study of the RegCM4's Surface Schemes in the Simulations of West Africa Climate. *Atmospheric Clim. Sci.* **2022**, *12*, 86–104. [CrossRef]
47. Paeth, H.; Hall, N.M.; Gaertner, M.A.; Alonso, M.D.; Moumouni, S.; Polcher, J.; Ruti, P.M.; Fink, A.H.; Gosset, M.; Lebel, T.; et al. Progress in regional downscaling of west African precipitation. *Atmos. Sci. Lett.* **2011**, *12*, 75–82. [CrossRef]
48. Paxian, A.; Sein, D.; Panitz, H.-J.; Warscher, M.; Breil, M.; Engel, T.; Tödter, J.; Krause, A.; Narvaez, W.D.C.; Fink, A.H.; et al. Bias reduction in decadal predictions of West African monsoon rainfall using regional climate models. *J. Geophys. Res. Atmos.* **2016**, *121*, 1715–1735. [CrossRef]
49. Dosio, A.; Panitz, H.-J. Climate change projections for CORDEX-Africa with COSMO-CLM regional climate model and differences with the driving global climate models. *Clim. Dyn.* **2015**, *46*, 1599–1625. [CrossRef]
50. Dieng, D.; Smiatek, G.; Bliefernicht, J.; Heinzeller, D.; Sarr, A.; Gaye, A.T.; Kunstmann, H. Evaluation of the COSMO-CLM high-resolution climate simulations over West Africa. *J. Geophys. Res. Atmos.* **2017**, *122*, 1437–1455. [CrossRef]
51. Müller, R.; Pfeifroth, U.; Träger-Chatterjee, C.; Trentmann, J.; Cremer, R. Digging the METEOSAT Treasure—3 Decades of Solar Surface Radiation. *Remote Sens.* **2015**, *7*, 8067–8101. [CrossRef]
52. Pfeifroth, U.; Sanchez-Lorenzo, A.; Manara, V.; Trentmann, J.; Hollmann, R. Trends and Variability of Surface Solar Radiation in Europe Based On Surface- and Satellite-Based Data Records. *J. Geophys. Res. Atmos.* **2018**, *123*, 1735–1754. [CrossRef]
53. Pal, J.S.; Small, E.E.; Eltahir, E.A.B. Simulation of regional-scale water and energy budgets: Representation of subgrid cloud and precipitation processes within RegCM. *J. Geophys. Res. Atmos.* **2000**, *105*, 29579–29594. [CrossRef]
54. Tiedtke, M. A comprehensive mass flux scheme for cumulus parameterization in large-scale models. *Mon. Weather Rev.* **1989**, *117*, 1779–1800. [CrossRef]
55. Kain, J.S.; Fritsch, J.M. A one-dimensional entraining/detraining plume model and its application in convective parameterization. *J. Atmos. Sci.* **1990**, *47*, 2784–2802. [CrossRef]
56. Holtslag, A.A.M.; De Bruijn, E.I.F.; Pan, H.L. A high resolution air mass transformation model for short-range weather forecasting. *Mon. Weather Rev.* **1990**, *118*, 1561–1575. [CrossRef]
57. Kiehl, J.T.; Hack, J.J.; Bonan, G.B.; Boville, B.A.; Briegleb, B.P.; Williamson, D.L.; Rasch, P.J. *Description of the NCAR Community Climate Model (CCM3)*; National Center for Atmospheric Research: Boulder, CO, USA, 1996.
58. Solmon, F.; Giorgi, F.; Liousse, C. Aerosol modelling for regional climate studies: Application to anthropogenic particles and evaluation over a European/African domain. *Tellus B Chem. Phys. Meteorol.* **2006**, *58*, 51. [CrossRef]
59. Zakey, A.S.; Solmon, F.; Giorgi, F. Implementation and testing of a desert dust module in a regional climate model. *Atmos. Meas. Tech.* **2006**, *6*, 4687–4704. [CrossRef]
60. Zakey, A.S.; Giorgi, F.; Bi, X. Modeling of sea salt in a regional climate model: Fluxes and radiative forcing. *J. Geophys. Res. Earth Surf.* **2008**, *113*. [CrossRef]
61. Lohmann, U.; Roeckner, E. Design and performance of a new cloud microphysics scheme developed for the ECHAM general circulation model. *Clim. Dyn.* **1996**, *12*, 557–572. [CrossRef]
62. Nordeng, T.E. *Extended Versions of the Convective Parametrization Scheme at ECMWF and Their Impact on the Mean and Transient Activity of the Model in the Tropics*; Technical Report No. 206; European Centre for Medium-Range Weather Forecasts: Reading, UK, 1994.
63. Pfeifer, S. Berichte Zur Erdsystemforschung. Modeling Cold Cloud Processes with the Regional Climate Model REMO. 2006. Available online: www.mpimet.mpg.de (accessed on 7 June 2022).
64. Louis, J.-F. A parametric model of vertical eddy fluxes in the atmosphere. *Bound.-Layer Meteorol.* **1979**, *17*, 187–202. [CrossRef]
65. Morcrette, J.J.; Smith, L.; Fourquart, Y. Pressure and temperature dependance of the absorption in longwave radiation parameterizations. *Beitr. Phys. Atmos.* **1986**, *59*, 455–469.

66. Giorgetta, M.; Wild, M. *The Water Vapour Continuum and Its Representation in Echam4*; Report No. 162; Max-Planck-Institute for Meteorology: Hamburg, Germany, 1995.
67. Tanre, D.; Geleyn, J.-F.; Slingo, J.M. *First Results of the Introduction of an Advanced Aerosol-Radiation Interaction in the ECMWF Low Resolution Global Model, Aerosols and Their Climatic Effects*; Gerber, H., Deepak, A., Eds.; Deepak Publ.: Hampton, VA, USA, 1984; pp. 133–177.
68. Doms, G.; Forstner, J.; Heise, E.; Herzog, H.-J.; Raschendorfer, M.; Schrodin, R.; Reinhardt, T.; Vogel, G. *A Description of the Nonhydrostatic Regional Model LM, Part II: Physical Parameterization*; Deutscher Wetterdienst: Offenbach, Germany, 2007.
69. Herzog, H.-J.; Schubert, U.; Vogel, G.; Fiedler, A.; Kirchner, R. *LLM—The High-Resolving Nonhydrostatic Simulation Model in the DWD-Project LITFASS. Part I: Modelling Technique and Simulation Method*; COSMO Technical Report No. 4; Deutscher Wetterdienst: Offenbach, Germany, 2002.
70. Ritter, B.; Geleyn, J.F. A comprehensive radiation scheme for numerical weather prediction models with potential applications in climate simulations. *Mon. Weather Rev.* **1992**, *120*, 303–325. [CrossRef]
71. Mavromatakis, F.; Makrides, G.; Georghiou, G.; Pothrakis, A.; Franghiadakis, Y.; Drakakis, E.; Koudoumas, E. Modeling the photovoltaic potential of a site. *Renew. Energy* **2010**, *35*, 1387–1390. [CrossRef]
72. Jerez, S.; Tobin, I.; Vautard, R.; Montávez, J.P.; López-Romero, J.M.; Thais, F.; Bartok, B.; Christensen, O.B.; Colette, A.; Déqué, M.; et al. The impact of climate change on photovoltaic power generation in Europe. *Nat. Commun.* **2015**, *6*, 10014. [CrossRef]
73. Bichet, A.; Hingray, B.; Evin, G.; Diedhiou, A.D.; Kebe, C.M.F.; Anquetin, S. Potential impact of climate change on solar resource in Africa for photovoltaic energy: Analyses from CORDEX-AFRICA climate experiments. *Environ. Res. Lett.* **2019**, *14*, 124039. [CrossRef]
74. Feron, S.; Cordero, R.R.; Damiani, A.; Jackson, R.B. Climate change extremes and photovoltaic power output. *Nat. Sustain.* **2020**, *4*, 270–276. [CrossRef]
75. Poddar, S.; Evans, J.P.; Kay, M.; Prasad, A.; Bremner, S. Estimation of future changes in photovoltaic potential in Australia due to climate change. *Environ. Res. Lett.* **2021**, *16*, 114034. [CrossRef]
76. Tonui, J.; Tripanagnostopoulos, Y. Performance improvement of PV/T solar collectors with natural air flow operation. *Sol. Energy* **2008**, *82*, 1–12. [CrossRef]
77. Chenni, R.; Makhlouf, M.; Kerbache, T.; Bouzid, A. A detailed modeling method for photovoltaic cells. *Energy* **2007**, *32*, 1724–1730. [CrossRef]
78. Emeis, S. *Wind Energy Meteorology: Atmospheric Physics for Wind Power Generation*; Springer: Berlin/Heidelberg, Germany, 2013.
79. Emeis, S. How well does a power law fit to a diabaticboundary-layer wind profile. *DEWI Mag.* **2005**, *26*, 59–62.
80. Hausfather, Z.; Peters, G.P. Emissions—The 'business as usual' story is misleading. *Nature* **2020**, *577*, 618–620. [CrossRef] [PubMed]
81. Riahi, K.; Rao, S.; Krey, V.; Cho, C.; Chirkov, V.; Fischer, G.; Kindermann, G.E.; Nakicenovic, N.; Rafaj, P. RCP 8.5—A scenario of comparatively high greenhouse gas emissions. *Clim. Change* **2011**, *109*, 33–57. [CrossRef]
82. Ehret, U.; Zehe, E.; Wulfmeyer, V.; Liebert, J. Should we apply bias correction to global and regional climate model data? *HESS* **2012**, *16*, 3391–3404.
83. Neher, I.; Crewell, S.; Meilinger, S.; Pfeifroth, U.; Trentmann, J. Photovoltaic power potential in West Africa using long-term satellite data. *Atmos. Meas. Tech.* **2020**, *20*, 12871–12888. [CrossRef]
84. Tall, M.; Albergel, C.; Bonan, B.; Zheng, Y.; Guichard, F.; Dramé, M.S.; Gaye, A.T.; Sintondji, L.O.; Hountondji, F.C.C.; Nikiema, P.M.; et al. Towards a Long-Term Reanalysis of Land Surface Variables over Western Africa: LDAS-Monde Applied over Burkina Faso from 2001 to 2018. *Remote Sens.* **2019**, *11*, 735. [CrossRef]
85. Dieng, D.; Cannon, A.J.; Laux, P.; Hald, C.; Adeyeri, O.; Rahimi, J.; Srivastava, A.K.; Mbaye, M.L.; Kunstmann, H. Multivariate Bias-Correction of High-Resolution Regional Climate Change Simulations for West Africa: Performance and Climate Change Implications. *J. Geophys. Res. Atmos.* **2022**, *127*. [CrossRef]
86. Seaby, L.; Refsgaard, J.; Sonnenborg, T.; Stisen, S.; Christensen, J.; Jensen, K. Assessment of robustness and significance of climate change signals for an ensemble of distribution-based scaled climate projections. *J. Hydrol.* **2013**, *486*, 479–493. [CrossRef]
87. Tebaldi, C.; Arblaster, J.M.; Knutti, R. Mapping model agreement on future climate projections. *Geophys. Res. Lett.* **2011**, *38*. [CrossRef]
88. Pirtle, Z.; Meyer, R.; Hamilton, A. What does it mean when climate models agree? A case for assessing independence among general circulation models. *Environ. Sci. Policy* **2010**, *13*, 351–361. [CrossRef]
89. Moemken, J.; Reyers, M.; Feldmann, H.; Pinto, J.G. Future changes of wind speed and wind energy potentials in EURO-CORDEX ensemble simulations MiKlip View project DFG-Project. *J. Geophys. Res. Atmos.* **2018**, *123*, 6373–6638. [CrossRef]
90. Deme, A.; Gaye, A.; Hourdin, F. Climate projections in West Africa: The obvious and the uncertain. In *Rural Societies in the Face of Climatic and Environmental Changes in West Africa*; Sultan, B., Lalou, R., Sanni, M., Oumarou, A., Soumare, M., Eds.; IRD Editions: Marseille, France, 2017; pp. 61–86.
91. Akinsanola, A.A.; Ogunjobi, K.; Abolude, A.T.; Salack, S. Projected changes in wind speed and wind energy potential over West Africa in CMIP6 models. *Environ. Res. Lett.* **2021**, *16*, 044033. [CrossRef]
92. Giorgi, F.; Francisco, R. Evaluating uncertainties in the prediction of regional climate change. *Geophys. Res. Lett.* **2000**, *27*, 1295–1298. [CrossRef]